Comparison of Wet and Dry Growth in Artificial and Flight Icing Conditions

R. John Hansman Jr.* and Mark S. Kirby†
Massachusetts Institute of Technology, Cambridge, Massachusetts

The heat transfer behavior of accreting ice surfaces in natural (flight test) and simulated (wind tunnel) cloud icing conditions are studied. Observations of wet and dry ice growth regimes as measured by ultrasonic pulse-echo techniques are made. Observed wet and dry ice growth regimes at the stagnation point of a cylinder are compared with those predicted using a quasi steady-state heat balance model. A series of heat transfer coefficients are employed by the model to infer the local heat transfer behavior of the actual ice surfaces. The heat transfer in the stagnation region is generally inferred to be higher in wind tunnel icing tests than in natural, flight icing conditions.

Nomenclature

A,B	= experimentally derived constants (−)
C_i	= specific heat capacity of ice, J/kg K
C_p	= specific heat capacity of air, J/kg K
C_w	= specific heat capacity of water, J/kg K
D	= diffusion coefficient of water vapor in air, m^2/s
d	= cylinder diameter, m
h	= local convective heat transfer coefficient, W/m^2K
k	= thermal conductivity of air, W/m K
L_f	= latent heat of fusion of water, J/kg
L_s	= latent heat of sublimation of water, J/kg
L_v	= latent heat of vaporization of water, J/kg
L^*	= effective latent heat of fusion
M''	= local mass flux/time, kg/m^2s
Nu	= Nusselt number (−)
Q''	= local heat flux/time, W/m^2
Re	= Reynolds number based on cylinder diameter and V_∞ (−)
r	= recovery factor, 0.875 (−)
ΔT_∞	= cloud supercooling = $-T_\infty$ (°C)
T_{surf}	= equilibrium surface temperature, °C
T_∞	= cloud temperature, °C
T^*	= effective surface freestream temperature difference, °C
t	= icing time, s
V_∞	= freestream velocity, m/s
W	= cloud liquid water content, g/m^3
β	= local collection efficiency (−)
$\rho_{v,surf}$	= saturated vapor density over surface, kg/m^3
$\rho_{v,\infty}$	= saturated vapor density in cloud, kg/m^3

I. Introduction

WHENEVER an aircraft encounters liquid moisture in the form of supercooled cloud or precipitation droplets, ice will form on the exposed surfaces. Depending on the ambient conditions, the ice growth may be either wet or dry. Dry growth occurs when the heat transfer from the accreting ice surface is adequate to remove all of the latent heat of the impinging droplets. The resulting ice shape typically protrudes forward into the airstream and is commonly referred to as "rime" ice (see Fig. 1). Wet growth occurs when the heat transfer from the surface is inadequate to remove all of the latent heat from the impinging droplets. The impinging droplets do not freeze on impact and may run back over the accreting surface as liquid water before freezing further downstream on the surface. This type of ice is commonly characterized as "glaze" ice, and often, the resulting ice shape displays two pronounced growth peaks on either side of the stagnation line (see Fig. 1). The most severe aircraft performance degradation is typically associated with glaze ice formations.[1] In some cases, both wet and dry ice growth can occur at different locations on the same body. This situation is referred to as "mixed" ice growth.

The physical processes which control ice accretion are distinctly different for dry and wet ice growth. In dry growth, where the droplets freeze on impact, the ice accretion is controlled by the local rate of impingement of liquid water on the surface. The local impinging mass flux is an inertially determined quantity which involves the individual droplet trajectories as they pass through the flowfield surrounding the body. For wet growth, the ice accretion is controlled by the rate at which latent heat of fusion can be removed from the surface. The heat transfer behavior of the ice surface, therefore, becomes the controlling mechanism for wet ice growth. For mixed icing conditions both the impingement and heat transfer mechanisms play important roles in the ice accretion process.

Efforts to analytically model the ice accretion process have been fairly successful for dry ice growth conditions where the thermodynamic analysis is trivial.[2] Experimental results have confirmed the accuracy of droplet trajectory calculations and predicted ice shapes are generally in good agreement with experimentally measured "rime" ice accretions.[3-5]

Analytical modeling of the ice accretion process for wet and mixed cases is significantly more difficult due to the need to evaluate both droplet trajectory and thermodynamic considerations and due to the potential for coupling between them. The primary area of uncertainty is in the convective heat transfer behavior of ice surfaces which is effectively an input parameter in the models. Due to experimental difficulties in instrumenting an actual accreting ice surface, no direct measurements have been made of the heat transfer from such surfaces and no direct validation of the thermodynamic models have been made. Even the most successful ice accretion models for wet conditions have a limited region of validity. In these models, the heat transfer

Received April 14, 1986; presented as Paper 86-1352 at the AIAA/ASME 4th Thermophysics and Heat Transfer Conference, Boston, MA, June 2-4, 1986; revision received July 28, 1986.

*Assistant Professor, Aeronautics and Astronautics. Member AIAA.
†Research Assistant, Aeronautics and Astronautics.

behavior of the surface is empirically inferred by adjusting the convective heat transfer coefficients until the ice shapes predicted by the models are in reasonable agreement with experimentally measured accretions.[6,7]

Recent development of ultrasonic ice accretion measurement techniques has allowed the detection of liquid water on an accreting ice surface.[8,9] The ability to determine if the ice growth is wet or dry allows a more direct evaluation of the thermodynamic models of the ice accretion process than has been previously possible. By parametrically identifying the transition between dry and wet ice growth, comparisons may be made between predicted and measured transition points in actual (flight test) and simulated (wind tunnel) icing conditions. By evaluating a series of candidate heat transfer coefficients in this manner some insight may be gained into the heat transfer behavior of surfaces under actual icing conditions.

In this paper, results of tests employing the ultrasonic technique on cylinders exposed to artificial icing conditions in the NASA Lewis Icing Research Tunnel (IRT) and natural icing conditions in flight from the NASA Lewis Twin Otter Icing Research Aircraft are presented. The results are analyzed in the context of a steady-state energy balance model in the stagnation region of the body. The study was limited to the stagnation region to avoid mass flux ambiguities which may occur in downstream locations due to water runback. A series of previously measured convective heat transfer coefficients with different levels of freestream turbulence and surface roughness[10] are used as inputs to the model.

II. Steady-State Thermodynamic Model for an Icing Surface

The thermodynamic analysis presented in this paper for a surface accreting ice follows the earlier work of Messinger[11] and others[12,13] and is commonly employed in current ice accretion models.[6,7] Figure 2 shows the principle modes of energy transfer associated with an icing surface. Heat is added to the surface primarily from the latent heat of fusion released as the droplets freeze, but also from aerodynamic heating and, to an even smaller extent, from the kinetic energy of the droplets impacting the surface. Heat is removed from the surface primarily by convection, and to a lesser degree by sublimation (when the surface is dry) or evaporation (when the surface is wet). In addition, heat is absorbed from the surface as the supercooled droplets impinge and warm to 0°C.

Figure 3 depicts the local control volume examined in this analysis. Since only the stagnation region of the body is considered in this paper, it is assumed that the only liquid entering the control volume is due to the impinging droplets. Liquid may, however, flow out of the control volume along the ice surface. Thus if the ice surface in the stagnation region is wet, insufficient heat is being removed to freeze all of the impinging liquid, and therefore the "freezing fraction" n is less than unity, where n is given by

$$n = \dot{M}''_{\text{frozen}} / \dot{M}''_{\text{impinging}} \tag{1}$$

The double prime superscript is used to indicate that the quantity is defined per unit area of the icing surface. When the ice surface is dry the freezing fraction is unity. The assumption of steady-state requires that the rate at which energy is added to the control volume equals the rate at which it is removed, i.e.,

$$\dot{Q}''_{\text{in}} = \dot{Q}''_{\text{out}} \tag{2}$$

where $\dot{Q}''_{\text{in}}$ and $\dot{Q}''_{\text{out}}$ represent the energy added to and removed from, respectively, the control volume per unit area per unit time. Equation (2) may be expanded into its component energy terms as

$$\dot{Q}''_{\text{in}} = \dot{Q}''_{\text{freezing}} + \dot{Q}''_{\text{aero heating}} + \dot{Q}''_{\text{droplet kinetic energy}} \tag{3}$$

$$\dot{Q}''_{\text{out}} = \dot{Q}''_{\text{conv}} + \dot{Q}''_{\text{sublimation/evaporation}} + \dot{Q}''_{\text{droplet warming}} \tag{4}$$

At steady-state it is assumed that the ice surface achieves a locally uniform equilibrium temperature, T_{surf}. Conduction into the ice is assumed to be zero and chordwise conduction between adjacent control volume is neglected. With these assumptions the component heat terms of Eqs. (3) and (4) may be written as

$$\left.\begin{aligned} \dot{Q}''_{\text{freezing}} &= \dot{M}''\,[L_f + C_i(0°\text{C} - T_{\text{surf}})] \\ \dot{Q}''_{\text{aero heating}} &= \frac{rhV_\infty^2}{2C_p} \\ \dot{Q}''_{\text{droplet kinetic energy}} &= \frac{\dot{M}''\,V_\infty^2}{2} \end{aligned}\right\} \dot{Q}''_{\text{in}} \tag{5a}$$

$$\left.\begin{aligned} \dot{Q}''_{\text{convection}} &= h(T_{\text{surf}} - T_\infty) \\ \dot{Q}''_{\text{sublimation/evaporation}} &= \frac{hDL_{s/v}}{k}(\rho_{v,\text{surf}} - \rho_{v,\infty}) \\ \dot{Q}''_{\text{droplet warming}} &= \dot{M}''\,C_w\Delta T_\infty \end{aligned}\right\} \dot{Q}''_{\text{out}} \tag{5b}$$

The local mass flux, $\dot{M}''$, of droplets impinging on a body in Eqs. (5a) and (5b) can be written as

$$\dot{M}'' = \beta W V_\infty \tag{6}$$

where W is the cloud liquid water content and β is the "local collection efficiency." It is defined as the ratio of the locally

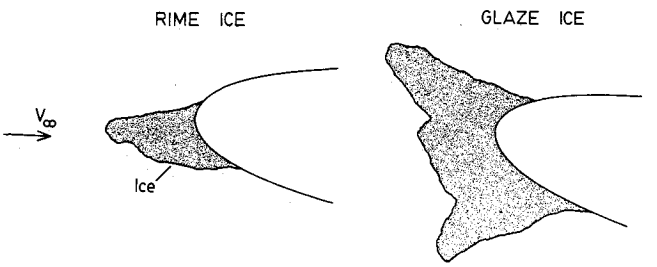

Fig. 1 Typical dry (rime) and wet (glaze) ice shapes.

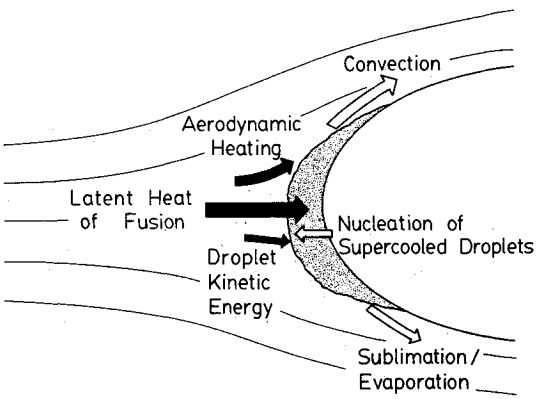

Fig. 2 Modes of energy transfer for an accreting ice surface.

impinging mass flux to the freestream mass flux, i.e.,

$$\beta = \frac{\text{locally impinging droplet flux}}{\text{freestream droplet flux}} \tag{7}$$

The local collection efficiency is an inertially determined quantity which involves the individual droplet trajectories as they pass through the flowfield surrounding the body. Because it is sensitive to the details of the flowfield and may be influenced by a variety of parameters, the local collection efficiency is normally evaluated by a droplet trajectory analysis around the body of interest.

The transition from dry to wet ice growth will occur when the equilibrium temperature of the surface rises to 0°C and the surface first starts to become wet. In this case the freezing fraction can be assumed to be unity although its actual value must be slightly lower.

The energy balance $\dot{Q}''_{\text{in}} = \dot{Q}''_{\text{out}}$ appropriate for the transition between dry and wet growth can be rewritten in terms of a "critical impinging liquid water content," $(\beta W)_{\text{crit}}$, given by

$$(\beta W)_{\text{crit}} = \frac{h[(0°\text{C} - T_\infty) + DL_v(\rho_{v,0°\text{C}} - \rho_{v,\infty})/k - rV_\infty^2/2C_p]}{V_\infty(L_f + V_\infty^2/2 - C_w\Delta T_\infty)} \tag{8}$$

Here the product $(\beta W)_{\text{crit}}$ is the wet/dry threshold and represents the critical locally impinging liquid water content necessary to produce a wet ice surface. If βW is greater than this critical value the ice surface will be wet and the freezing fraction will be less than one, while if βW is less than this critical value the ice surface will be dry. From this equation it can be seen that $(\beta W)_{\text{crit}}$ depends on the assumed values of the convective heat transfer coefficient h.

It is convenient to express the convective heat transfer coefficient in terms of the dimensionless Nusselt number, Nu, where

$$Nu = hd/k \tag{9}$$

with d being the uniced diameter or characteristic dimension of the body, and k the thermal conductivity of air. Experimental measurements of local heat transfer coefficient distributions are often presented in terms of a power-law relationship between the Nusselt number and the Reynolds number

$$Nu = ARe^B = A(\rho_\infty V_\infty d/\mu_\infty)^B \tag{10}$$

where A and B are experimentally derived constants.

Using Eqs. (9) and (10), the critical impinging liquid water current Eq. (8) may be rewritten as

$$(\beta W)_{\text{crit}} = Ak(\rho_\infty/\mu_\infty)^B (V_\infty d)^{B-1}(T^*/L^*) \tag{11}$$

The constants A and B represent the convective heat transfer coefficient "model," or power law. The terms T^* and L^* introduced in Eq. (11) are defined below as

$$T^* = [(0°\text{C} - T_\infty) + DL_v(\rho_{v,0°\text{C}} - \rho_{v,\infty})/k - rV_\infty^2/2C_p] \tag{12}$$

$$L^* = [L_f + V_\infty^2/2 - C_w\Delta T_\infty] \tag{13}$$

The term T^* can be thought of as representing the effective temperature difference between the icing surface and the freestream. This effective temperature difference controls the rate at which heat is removed from the icing surface by convection and evaporation. The effect of aerodynamic heating is also included in this temperature difference term.

In a similar way, the term L^* represents an effective heat of fusion released during the accretion process. This term combines the latent heat of fusion of water L_f, the droplet specific kinetic energy $V_\infty^2/2$, and the effective heat absorbed due to droplet warming on impact $C_w\Delta T_\infty$. Since the droplet kinetic energy and droplet warming terms are typically an order of magnitude smaller than the latent heat of fusion of water, the parameter L^* is, in most cases, essentially equal to L_f.

From Eq. (11) it can be seen that $(\beta W)_{\text{crit}}$ depends on the assumed values of A and B in the heat transfer coefficient model. By measuring the locally impinging liquid water content, βW, and whether the resulting ice surface is wet or dry, it is thus possible to compare different heat transfer models and determine which physical model best predicts the observed wet or dry ice growth.

III. Ultrasonic Pulse-Echo Analysis of an Accreting Ice Surface

Figure 4 illustrates the principle of the ultrasonic pulse-echo measurement technique applied for an icing surface.[8] A small transducer mounted flush with the accreting surface emits a brief compressional wave, the ultrasonic pulse travels through the ice as shown. This wave is reflected at the external ice surface and returns to the emitting transducer as an echo signal. By measuring the time elapsed between the emission of the pulse and the return of the echo, the ice thickness over the transducer may be calculated using the appropriate speed of sound for ice (3.8 mm/μs). Prior studies have

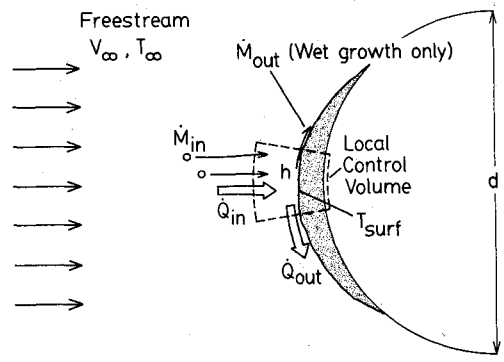

Fig. 3 Stagnation region control volume used for steady-state thermodynamic analysis.

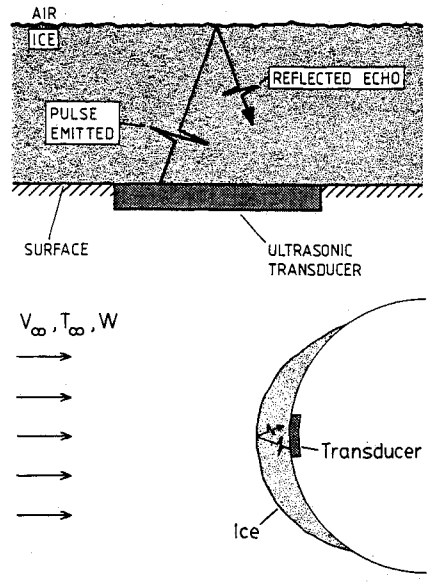

Fig. 4 Ultrasonic pulse-echo measurement technique.

found the speed of sound to be relatively insensitive to ice-type for typical aircraft accretions.[8] By repeatedly emitting pulses the ice thickness can be constantly measured as ice accretes on the body.

In addition to obtaining the ice thickness from the pulse-echo transit time, the condition of the ice surface may also be monitored via the characteristics of the ultrasonic echo pattern received from the ice surface. Specifically, it has been found[9] that the echo patterns received from a dry ice surface and a wet ice surface are markedly different. A single echo, corresponding to the ice/air interface over the transducer, is received from a dry ice surface. However, during wet ice growth, the presence of liquid water on the ice surface creates a different, reflective interface, namely that between liquid and air. Thus, during wet ice growth, the received echo pattern contains an echo from the ice/water interface, as well as rapidly varying echoes from the water/air interface. The presence of these echoes, which vary due to the distortion of the water by the impinging droplets and flowfield, is used to determine if the ice growth is wet. If only a single echo is received from the ice surface, then the ice growth is determined to be dry.

IV. Experimental Facilities and Test Description

A. Icing Research Tunnel Tests

A series of tests was performed in the NASA Lewis Research Center Icing Research Tunnel (IRT). A 0.102 m (4.0 in.) diameter cylinder instrumented with ultrasonic transducers was suspended vertically from the top of the icing tunnel as shown in Fig. 5. The transducers were located on the stagnation line of the cylinder. The echo signals received from these transducers were displayed on an oscilloscope. The oscilloscope screen was videotaped to provide a permanent record of the time-dependent echo patterns. The test procedure consisted of lowering the tunnel temperature to the desired icing cloud condition with the water spray off. Once the tunnel temperature had stabilized, the water spray system was turned on to produce a cloud of droplets of the desired size (median volume diameter). Typically, the spray system was activated for a six minute period, after which it was turned off. Photographic and other measurements of the iced cylinder were then made and the cylinder was completely deiced before the start of the next run. A total of 36 runs for 15 different icing conditions were performed.

B. Natural Icing Tests

A second series of tests was performed in natural icing conditions using a 0.114 m (4.5 in.) diameter cylinder similarly instrumented with ultrasonic transducers on the stagnation line. An oscilloscope was again used to display the received echo signals which were videotaped as before. The cylinder was exposed to the icing cloud via an experiment carrier mounted in the roof of the NASA Lewis Icing Research Aircraft (De Havilland Twin Otter), shown in Fig. 6. When deployed, the cylinder was located 0.53 m (21 in.) into the freestream above the roof-line of the aircraft. The cylinder was exposed throughout the icing encounter, which typically lasted approximately 20 minutes. Throughout the exposure, other instruments mounted on the research aircraft measured aircraft and icing cloud parameters. In particular, a Johnson-Williams hot-wire probe was used to record cloud liquid water content and a forward scattering laser probe (FSSP) was used to measure the cloud droplet size distribution. Four separate exposures were conducted in this series of flight tests.

V. Experimental Results and Discussion

The limited time available for testing in the icing research tunnel and the research aircraft prevented a precise determination of the stagnation heat transfer coefficients by means of the experimentally measured wet or dry ice growths alone. However, the wet/dry ice growth data obtained could be used to compare the ice growth predicted by different heat transfer coefficients in the form $Nu = A\ Re^B$ and the quasi steady-state icing model. Recent experimental heat transfer coefficient measurements about a bare cylinder by Van Fossen et al.,[10] in support of the NASA icing research program are compared in this way. The bare cylinder is considered because most of the wet/dry measurements were obtained for relatively small ice thicknesses, and hence, for flowfield purposes, the geometry is essentially that of a bare cylinder.

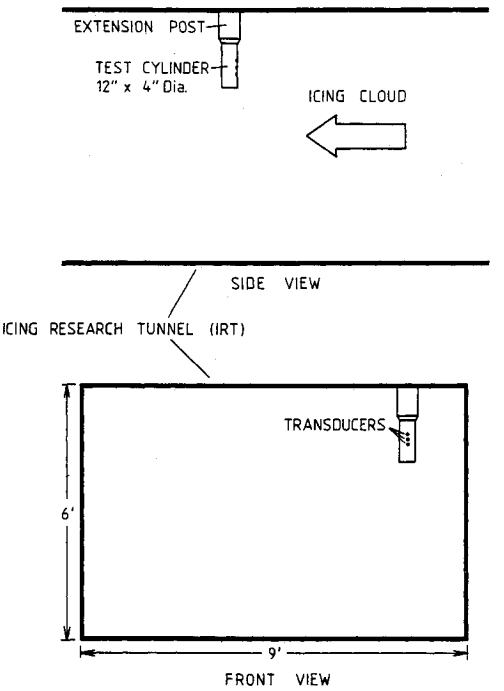

Fig. 5 Test cylinder installation for icing research tunnel (IRT) tests.

In the Van Fossen et al. study,[10] heat transfer coefficients were measured for two different freestream turbulence levels, 0.5% and 3.5%, and for two different cylinder surface conditions, one smooth and one roughened with grains of sand, with an average element height of 0.33 mm. The 0.5% freestream turbulence level was the minimum turbulence level achievable in the Van Fossen tests. The 3.5% turbulence was chosen to characterize the higher turbulence level believed to exist in the icing research tunnel.

The stagnation region heat transfer coefficient was found by Van Fossen et al., to increase both with freestream turbulence level and with surface roughness. This behavior has been observed in separate studies[14,15] at Reynolds numbers similar to those encountered in the test program (400,000-900,000).

A. Icing Research Tunnel Results

Figure 7 shows the ultrasonically measured ice growth for six different icing conditions observed in the icing research tunnel. The freestream velocity was 102.8 m/s (230 mph) for all six runs shown corresponding to a typical Reynolds number of 875,000. The impinging liquid water content βW was determined directly from the ultrasonically measured dry ice growth accretion rate, since for dry growth the freezing fraction is unity.

Figure 7 also shows four wet/dry threshold curves calculated using the Van Fossen et al. heat transfer values. These curves are plotted versus ambient temperature and were calculated for the experimental values of cylinder diameter and freestream velocity. The four curves shown

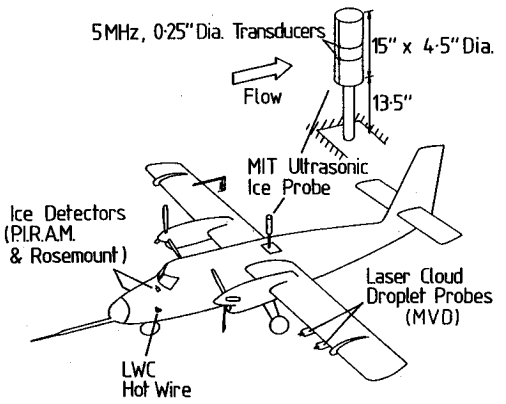

Fig. 6 Test cylinder installation for natural icing flight tests on the NASA, Twin Otter, Icing Research Aircraft.

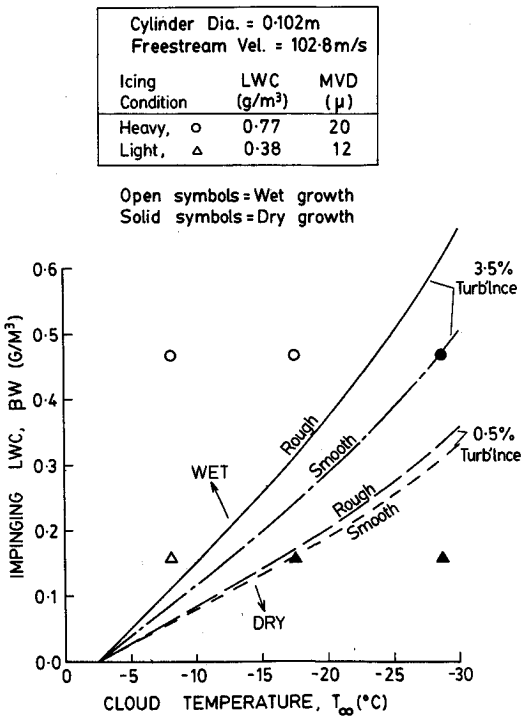

Fig. 7 Plot of impinging liquid water content versus cloud temperature showing ultrasonically measured wet/dry ice growth and theoretical wet/dry threshold curves for four different heat transfer coefficient [V_∞ = 102.8 m/s, (230 mph)].

thus represent the transition line between wet and dry ice growth calculated for the four different local heat transfer coefficients implied by the Van Fossen data. If the local impinging liquid water content exceeds this value of $(\beta W)_{crit}$ for a given ambient temperature then the ice growth is expected to be wet, and if βW is less than $(\beta W)_{crit}$, the ice growth is predicted to be dry. From the figure, it can be seen that the curve which best predicts the experimentally observed pattern of wet and dry ice growth is that which corresponds to the cylinder roughened with sand at a freestream turbulence level of 3.5%. The curves corresponding to the low (0.5%) turbulence level clearly underpredict the heat transfer observed in this case.

Figure 8 presents wet/dry ice growth measurements for two additional freestream velocities of 71.5 m/s (160 mph) and 49.2 m/s (110 mph) corresponding to Reynolds numbers

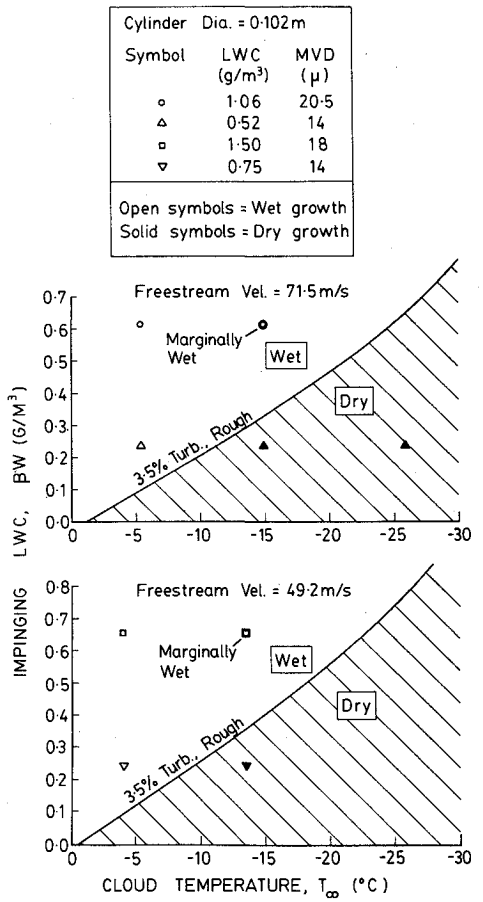

Fig. 8 Plot of impinging liquid water content versus cloud temperature showing ultrasonically measured wet/dry ice growth at two additional freestream velocities and the theoretical wet/dry threshold curve corresponding to the 3/5% turbulence level, rough surface, heat transfer coefficient of Van Fossen et al.

of approximately 610,000 and 420,000, respectively. The impinging liquid water content βW was obtained from the dry growth accretion rate, where available, or by calculation of β for those cases where only wet or marginally wet ice growth was observed. The wet/dry threshold curves calculated using the high heat transfer data (3.5% turbulence level, rough) of Van Fossen et al. are also shown.

The observed pattern of wet and dry growth in the IRT is consistent with the highest heat transfer Van Fossen et al. data. In addition, the two marginally wet cases observed suggest that the heat transfer over the ice surface in the stagnation region may in fact be even greater than that implied by the 3.5% turbulence data of Van Fossen. Based on the results presented in Figs. 7 and 8, the observed behavior in the IRT is consistent with a relatively high convective heat transfer coefficient equal to or greater than the highest Nusselt number model of Van Fossen et al. corresponding to a 3.5% turbulence level rough surface.

Note that only the heat transfer behavior at the stagnation region has been evaluated in the above analysis. The stagnation heat transfer is affected by both the freestream turbulence level and the surface roughness. It is possible to get similar heat transfer behavior with a variety of surface roughness, turbulence level combinations. Therefore, even though the heat transfer is similar, it is likely that the actual conditions encountered in the IRT varied somewhat from the 3.5% turbulence level, 0.33 mm sand grain roughness observed by Van Fossen et al.

An additional qualification is that the IRT measurements were limited to the stagnation region due to water runback which creates uncertainty as to the mass flux in the

downstream regions. The local heat transfer coefficient in the stagnation region is less sensitive to the surface roughness than to the freestream turbulence level, as can be seen from the four curves in Fig. 7. However, local surface roughness does play a critical role in determining where boundary layer transition occurs.[14] This, in turn, significantly affects the heat transfer distribution around the body and therefore the resulting ice shape. Accurate analytic models of the local surface roughness on real iced surfaces have not yet been developed; however, the local surface roughness has been found to vary with both position on the body and the icing conditions under which the ice was formed.[15] Thus, while the heat transfer coefficient implied by the rough surface, 3.5% turbulence level measurements appears to best predict the experimentally observed pattern of wet and dry ice growth, this heat transfer behavior may be applicable only to the stagnation region, and different values may apply elsewhere on the cylinder.

B. Natural Icing Cloud Test Results

While constant icing conditions were maintained throughout each exposure in the icing research tunnel, the natural icing cloud conditions, most noticeably the liquid water content, were not constant throughout each flight. Figure 9 shows a plot of cloud liquid water content versus exposure time for research flight 85-24. The liquid water content was measured by a Johnson-Williams hot-wire probe located near the nose of the aircraft (see Fig. 6). Also shown are the experimentally observed periods of dry, wet, and transitional ice growth produced by the varying impinging liquid water content. The ultrasonic echo patterns received from the accreting ice surface were used to determine if the ice growth was wet, dry, or transitional. Ice growth was characterized as transitional when the ultrasonic echoes received from the ice surface displayed neither predominantly dry nor wet echo patterns.

Since the thermodynamic model used to compare heat transfer coefficients assumes a quasi steady-state icing process, and since the cloud liquid water content varied significantly throughout each exposure, a simple, steady-state time constant was estimated. This time constant was then applied as a criteria for comparing the ultrasonic data with the wet/dry growth regimes predicted by the steady-state model. A time constant of ten seconds was selected based on the transient thermal response of a thin ice layer and on the time response of the Johnson-Williams liquid water content measurements. Therefore, only liquid water content levels sustained for greater than 10 seconds were used in the categorization of ice growth as wet, dry, or transitional.

Figure 10 is a plot of impinging liquid water content versus cloud temperature. The experimentally observed ice growth regimes during the four research flights conducted are shown. Note that during flights 85-24 and 85-25 the full range of ice growth regimes were encountered with periods of dry, transitional, and wet ice growth observed. No dry ice growth was observed during flights 85-22 and 85-23. Also shown are the four wet/dry threshold curves calculated using the four different Van Fossen heat transfer coefficients (0.5% turbulence, rough, and smooth surface; 3.5% turbulence, rough, and smooth surface). These curves were calculated for the average test conditions of cylinder diameter 0.114 m (4.5 in.), flight airspeed of 71.4 m/s (160 mph), exposure attitude of 1613 m (5300 ft) and a typical Reynolds number of 650,000.

Figures 9 and 10 illustrate the considerable variations encountered in natural icing conditions, both during a particular flight and between flights conducted on different days. For example, the cloud temperature, liquid water content and droplet size were roughly comparable for flights 85-24 and 85-25. However, different ranges of wet and dry ice growth were observed, as indicated by the overlapping observed wet and dry growth ranges at the same impinging liquid water content. The implication is that the heat transfer differed between the two flights, both at nominally similar icing conditions, but conducted on different days through different clouds.

From Fig. 10 it can be seen that for flight 85-25 the high heat transfer curves corresponding to the Van Fossen et al. 3.5% turbulence level data overpredict the observed heat transfer, based on the steady-state analysis. For this flight, the lower heat transfer curves corresponding to the 0.5% turbulence data correctly predict the observed wet and dry regimes. The actual heat transfer could be even lower based on the location of the observed wet and dry growth regimes.

In contrast to flight 85-25, the observed ice growth regimes during flight 85-24 are consistent with the wet/dry threshold predicted by the higher (3.5% turbulence level) heat transfer

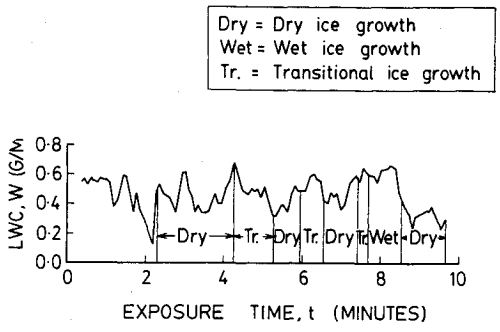

Fig. 9 Plot of liquid water content (measured by the Johnson-Williams probe) versus exposure time for flight 85-24 showing typical fluctuations observed in natural icing conditions. Also shown are ultrasonic measured periods of wet, dry, and transitional ice growth.

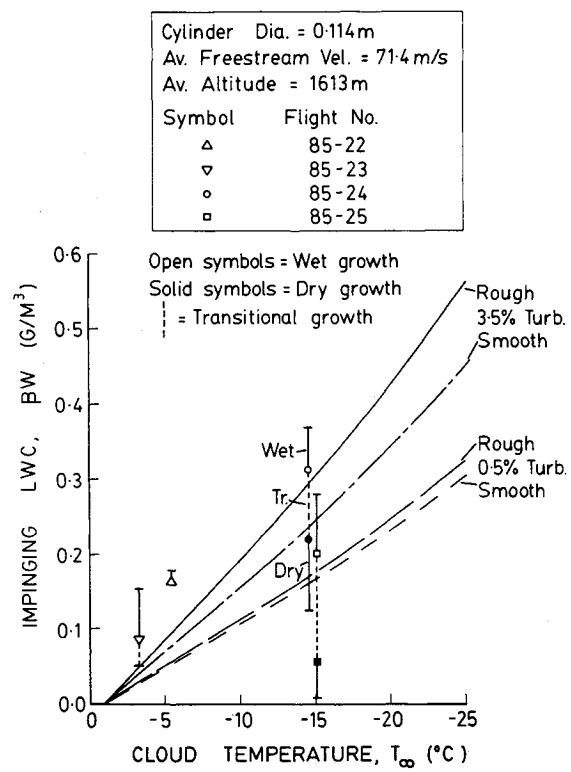

Fig. 10 Plot of impinging liquid water content versus cloud temperature showing wet, dry, and transitional ice growth regimes observed in flights and theoretical wet/dry threshold curves for four different heat transfer coefficients.

data. For this flight, the lower heat transfer in the 0.5% turbulence level curves incorrectly predict wet growth for impinging liquid water content levels where dry growth was experimentally observed. There appears, therefore, to be a significant variation in the heat transfer behavior for these two flights despite nominally similar icing conditions.

The results of these tests highlight the effect of variations in icing conditions which are inherent in all natural icing encounters. Ice growth may thus vary from wet to dry during a particular encounter as the impinging liquid water content fluctuates. The ice shapes formed during pure dry (rime ice) or pure wet (glaze ice) growth are markedly different (see Fig. 1). Therefore, the use of an average cloud liquid water content to represent a particular natural icing encounter may be inappropriate since this will imply either pure wet or pure dry growth, when in reality the ice growth (wet or dry) often varies as a function of time.

The results of the natural icing tests also indicate the heat transfer occurring in natural icing conditions may vary from day to day despite similar icing conditions. One reason for this variation may be due to different icing cloud turbulence levels. Based on the limited amount of flight test data available it appears that in general the appropriate heat transfer coefficient for natural icing conditions is somewhat lower than the level inferred for the icing research tunnel. This result is consistent with previous experimental comparisons between the icing research tunnel and flight by Gelder and Lewis.[17] Note that the high heat transfer observed in the IRT is likely due to turbulence introduced into the tunnel by the droplet spray system. This problem is generic to all icing simulation facilities where droplets must be injected into the flow. For these reasons, care should be taken in extrapolating the results of icing wind tunnel tests to similar natural icing cloud conditions.

VI. Conclusions

Results of tests conducted in artificial (icing research tunnel) and natural (flight) icing conditions have shown the following:

1) The presence of liquid water on an accreting surface may be detected using an ultrasonic pulse-echo technique.

2) The threshold between dry and wet ice growth can be theoretically determined if the local convective heat transfer coefficient is known.

3) By comparing experimentally measured wet or dry ice growth with wet/dry thresholds predicted by different heat transfer coefficients, it is possible to infer heat transfer behavior for an iced surface in icing conditions.

4) The stagnation region heat transfer occurring during initial ice growth in the icing research tunnel appears to be relatively high. The observed wet/dry growth patterns are consistent with a convective heat transfer coefficient which equals or exceeds the Van Fossen et al. 3.5% freestream turbulence level, rough surface heat transfer model for a bare cylinder.

5) During natural icing cloud encounters, conditons are not constant and, as a result, periods of wet, dry, and transitional ice growth may be observed within a single encounter.

6) The heat transfer occurring during initial ice growth in natural icing conditions has been inferred to vary significantly from flight to flight. However, on average, the heat transfer in natural conditions tends to be somewhat lower than in artificial icing conditions.

7) Because of variations in natural icing cloud conditions, care should be taken in extrapolating results from icing wind tunnels to similar natural icing cloud conditions.

Acknowledgments

This work was supported by the National Aeronautics and Space Administration and the Federal Aviation Administration under Grant NGL-22-009-640 and NAG3-666. Wind tunnel and flight test facilities were provided by the NASA Lewis Research Center.

References

[1]Ranaudo, R.J., Mikkelsen, K.L., McKnight, R.C., and Perkins, P.J., Jr., "Performance Degradation of a Typical Twin Engine Commuter Type Aircraft in Measured Natural Icing Conditions," NASA TM-83564, 1984.

[2]Bragg, M.B., Gregorek, G.M., and Shaw, R.J., "Analytical Approach to Airfoil Icing," AIAA Paper 81-0403, Jan. 1981.

[3]Brun, R.J. and Mergler, H.W., "Impingement of Water Droplets on a Cylinder in an Incompressible Flow Field and Evaluation of Rotating Multicylinder Method for Measurement of Droplet-Size Distribution, Volume-Median Droplet Size, and Liquid-Water Content in Clouds," NACA TN2904, March 1953.

[4]Gelder, T.F., Smyers, W.H., Jr., and von Glahn, U., "Experimental Droplet Impingement on Several Two-Dimensional Airfoils with Thickness Ratios of 6 to 16 Percent," NACA TN3839, Dec. 1956.

[5]Hansman, R.J., "The Effect of the Atmospheric Droplet Size Distribution on Aircraft Ice Accretion," AIAA Paper 84-0108, Jan. 1984.

[6]Cansdale, J.T. and Gent, R.W., "Ice Accretion on Aerofoils in Two-Dimensional Compressible Flow-A Theoretical Model," RAE TR 82128, 1983.

[7]MacArthur, C.D., Keller, J.L., and Leurs, J.K., "Mathematical Modeling of Ice Accretions on Airfoils," AIAA Paper 82-0284, Jan. 1982.

[8]Hansman, R.J. and Kirby, M.S., "Measurement of Ice Accretion Using Ultrasonic Pulse-Echo Techniques," *Journal of Aircraft,* Vol. 22, June 1985, pp. 530–535.

[9]Hansman, R.J. and Kirby, M.S., "Measurement of Ice Growth During Simulated and Natural Icing Conditions Using Ultrasonic Pulse-Echo Techniques," *Journal of Aircraft,* Vol. 23, June 1986, pp. 492–498.

[10]Van Fossen, G.J., Simoneau, R.J., Olsen, W.A., and Shaw, R.J., "Heat Transfer Distributions Around Nominal Ice Accretion Shapes Formed on a Cylinder in the NASA Lewis Icing Research Tunnel," AIAA Paper 84-0017, Jan. 1984.

[11]Messinger, B.L., "Equilibrium Temperature of an Unheated Icing Surface as a Function of Airspeed," *Journal of the Aeronautical Sciences,* Jan. 1953, pp. 24–42.

[12]Ludlam, F.H., "The Heat Economy of a Rimed Cylinder," *Quarterly Journal of the Royal Meteorological Society,* Vol. 77, 1951, pp. 663–666.

[13]Macklin, W.C. and Payne, G.S., "A Theoretical Study of the Ice Accretion Process," *Quarterly Journal of the Royal Meteorological Society,* Vol. 93, 1967, pp. 195–213.

[14]Achenbach, E., "The Effect of Surface Roughness on the Heat Transfer from a Circular Cylinder to the Cross Flow of Air," *International Journal of Heat Mass Transfer,* Vol. 20, 1977, pp. 359–369.

[15]Smith, M. and Kuethe, A., "Effects of Turbulence on Laminar Skin Friction and Heat Transfer," *The Physics of Fluids,* Vol. 9, No. 12, 1966, pp. 2337–2344.

[16]Olsen, W., Shaw, R., and Newton, J., "Ice Shapes and the Resulting Drag Increase for an NACA 0012 Airfoil," NASA TN83556, 1984.

[17]Gelder, T.F. and Lewis, J.P., "Comparison of Heat Transfer From an Airfoil in Natural and Simulated Icing Conditions," NACA TN2480, Sept. 1951.